Title

Myb-like transcription factors have epistatic effects on circadian clock function but additive effects on plant growth

Journal

Plant Direct, 7(10)

ISSN

2475-4455

Authors

Hughes, Cassandra L

Harmer, Stacey L

Publication Date

2023-10-01

DOI

10.1002/pld3.533

Peer reviewed

Received: 22 May 2023 | Revised: 23 August 2023 | Accepted: 4 September 2023

DOI: 10.1002/pld3.533

RESEARCH ARTICLE

Myb-like transcription factors have epistatic effects on circadian clock function but additive effects on plant growth

Cassandra L. Hughes | **Stacey L. Harmer**

Department of Plant Biology, University of California, Davis, California, USA

Correspondence
Stacey L. Harmer, Department of Plant Biology, University of California, Davis, CA, USA.
Email: slharmer@ucdavis.edu

Funding information
National Institutes of Health, Grant/Award Number: R01 GM069418; US Department of Agriculture-National Institute of Food and Agriculture, Grant/Award Number: CA-D-PLB-2259-H

Abstract

The functions of closely related Myb-like repressor and Myb-like activator proteins within the plant circadian oscillator have been well-studied as separate groups, but the genetic interactions between them are less clear. We hypothesized that these repressors and activators would interact additively to regulate both circadian and growth phenotypes. We used CRISPR-Cas9 to generate new mutant alleles and performed physiological and molecular characterization of plant mutants for five of these core Myb-like clock factors compared with a repressor mutant and an activator mutant. We first examined circadian clock function in plants likely null for both the repressor proteins, *CIRCADIAN CLOCK ASSOCIATED 1* (*CCA1*) and *LATE ELONGATED HYPOCOTYL* (*LHY*), and the activator proteins, *REVEILLE 4* (*RVE4*), *REVEILLE* (*RVE6*), and *REVEILLE* (*RVE8*). The *rve468* triple mutant has a long period and flowers late, while *cca1 lhy rve468* quintuple mutants, similarly to *cca1 lhy* mutants, have poor circadian rhythms and flower early. This suggests that *CCA1* and *LHY* are epistatic to *RVE4*, *RVE6*, and *RVE8* for circadian clock and flowering time function. We next examined hypocotyl elongation and rosette leaf size in these mutants. The *cca1 lhy rve468* mutants have growth phenotypes intermediate between *cca1 lhy* and *rve468* mutants, suggesting that *CCA1*, *LHY*, *RVE4*, *RVE6*, and *RVE8* interact additively to regulate growth. Together, our data suggest that these five Myb-like factors interact differently in regulation of the circadian clock versus growth. More generally, the near-norm al seedling phenotypes observed in the largely arrhythmic quintuple mutant demonstrate that circadian-regulated output processes, like control of hypocotyl elongation, do not always depend upon rhythmic oscillator function.

KEYWORDS
Arabidopsis thaliana; *CCA1*, *LHY*; flowering time; hypocotyl elongation; *RVE4*, *RVE6*, *RVE8*

1 | INTRODUCTION

The circadian clock is a biological timekeeper that allows organisms to anticipate predictable daily changes in the environment and regulate their responses to stimuli depending on the time of day. This helps an organism synchronize its physiology with its surroundings, providing a fitness advantage (Dodd et al., 2005; Ouyang et al., 1998; Spoelstra et al., 2016). The importance of circadian clocks is further supported by their presence in diverse eukaryotes and some prokaryotes. Although specific circadian clock components are not conserved

across higher taxa, clocks in eukaryotes are composed of interlocking transcriptional-translational feedback loops (Hsu & Harmer, 2014; Rosbash, 2009).

In plants, a family of Myb-like transcription factors is part of the core circadian clock and is highly conserved across land plants. Subclades in this family include one group of proteins that act primarily as repressors and one group of proteins that act primarily as activators. These factors bind to the same *cis*-element sequences and act antagonistically to each other (Alabadí et al., 2001; Harmer & Kay, 2005; Hsu et al., 2013; Rawat et al., 2011). In *A. thaliana*, *CIRCADIAN CLOCK ASSOCIATED 1* (*CCA1*) and *LATE ELONGATED HYPOCOTYL* (*LHY*) are morning-phased Myb-like repressors that repress expression of *TIMING OF CAB EXPRESSION 1* (*TOC1*), *PSEUDO-RESPONSE REGULATOR 5* (*PRR5*), *PSEUDO-RESPONSE REGULATOR 7* (*PRR7*), and *PSEUDO-RESPONSE REGULATOR 9* (*PRR9*) (Alabadí et al., 2001; Kamioka et al., 2016). These pseudo-response regulator proteins then reciprocally repress expression of *CCA1* and *LHY* (Gendron et al., 2012; Huang et al., 2012; Nakamichi et al., 2010). CCA1 and LHY also repress expression of the evening complex genes *EARLY FLOWERING 3* (*ELF3*), *EARLY FLOWERING 4* (*ELF4*), and *LUX ARRHYTHMO* (*LUX*) (Adams et al., 2018; Hazen et al., 2005; Kamioka et al., 2016; Li et al., 2011; Nagel et al., 2015). *REVEILLE 4* (*RVE4*), *REVEILLE 6* (*RVE6*), and *REVEILLE 8* (*RVE8*) encode Myb-like transcription factors that act in opposition to CCA1 and LHY to activate expression of these same targets (Farinas & Mas, 2011; Hsu et al., 2013; Rawat et al., 2011). Considering these two groups of repressors and activators together, these atypical Myb-like factors are involved in all main transcription-translation feedback loops that compose the core clock (Creux & Harmer, 2019; Davis et al., 2022).

Most of the core components of the plant circadian oscillator are transcription factors, which in addition to controlling each other's expression regulate genes involved in diverse physiological processes such as flowering time and growth. CCA1, LHY, PRR5, PRR7, and PRR9 indirectly regulate *CONSTANS* (*CO*) expression (Fornara et al., 2009; Nakamichi et al., 2012; Niwa et al., 2007), and the CO protein activates expression of *FLOWERING LOCUS T* (*FT*) to promote flowering (Kardailsky et al., 1999; Kobayashi et al., 1999). The evening complex (ELF3, ELF4, and LUX) directly represses expression of *PHYTOCHROME INTERACTING FACTOR 4* (*PIF4*) and *PHYTOCHROME INTERACTING FACTOR 5* (*PIF5*) (Nusinow et al., 2011), genes that encode bHLH transcription factors that promote elongation of multiple plant organs. Adding another layer of regulation by the circadian clock, the activity of PIF proteins is modulated by their direct binding to TOC1 and the related proteins PRR5, PRR7, and PRR9 (Martín et al., 2018; Soy et al., 2016; Zhang et al., 2020). PIF4 and PIF5 promote hypocotyl elongation at least in part by promoting expression of auxin biosynthesis genes (Franklin et al., 2011; Hornitschek et al., 2012; Koini et al., 2009; Kunihiro et al., 2011; Nozue et al., 2011; Sun et al., 2012). As illustrated by these examples, circadian clock factors directly and indirectly regulate expression of genes that in turn control a wide range of important physiological processes. This complexity makes it difficult to determine whether the phenotypes of plants mutant for core clock genes are due to alterations in circadian rhythmicity per se or due to mis-regulation of downstream target genes.

As might be expected of factors with antagonistic effects on gene expression, *cca1 lhy* and *rve468* mutants have several opposite mutant phenotypes. Plants mutant for the repressors *CCA1* and *LHY* have short-period circadian rhythms, shorter hypocotyls and smaller leaves, and flower earlier than wild type (Alabadí et al., 2002; Hall et al., 2003; Locke et al., 2005; Más et al., 2003; Mizoguchi et al., 2002; Niwa et al., 2007). Plants mutant for the *RVE4*, *RVE6*, and *RVE8* activators have long-period circadian rhythms, longer hypocotyls and larger leaves, and flower later than wild type (Gray et al., 2017; Hsu et al., 2013; Rawat et al., 2011). *PIF4* and *PIF5* are required for the large rosette phenotype observed in *rve468* mutants (Gray et al., 2017).

Although *CCA1*, *LHY*, *RVE4*, *RVE6*, and *RVE8* mutants have been extensively characterized, the relationship between these repressors and activators both in the circadian clock and in regulation of plant growth remains unclear. The partial loss-of-function *cca1-1 lhy-20 rve4-1 rve6-1 rve8-1* mutants are highly rhythmic with an approximate 24-h period in optimal growth conditions and are more phenotypically similar to wild-type plants than *cca1 lhy* or *rve4 rve6 rve8* mutants (Shalit-Kaneh et al., 2018). This is surprising given that *CCA1*, *LHY*, *RVE4*, *RVE6*, and *RVE8* are integral for normal clock function (Alabadí et al., 2002; Farinas & Mas, 2011; Green & Tobin, 1999; Hsu et al., 2013; Mizoguchi et al., 2002; Rawat et al., 2011; Wang & Tobin, 1998). However, rhythmicity is greatly reduced in quintuple *cca1 lhy rve468* mutants maintained at non-optimal temperatures (Shalit-Kaneh et al., 2018), suggesting that collectively the Myb-like factors act to increase circadian robustness and enhance adaptation to challenging growth conditions.

Because the previously studied *cca1 lhy rve468* mutant was not a null mutant (Shalit-Kaneh et al., 2018), we wanted to determine if the clock remains robustly rhythmic in the complete absence of these five core factors. Here, we report the characterization of CRISPR-Cas9-generated alleles of *RVE4*, *RVE6*, and *RVE8* and their phenotypes alone and in combination with mutations in *CCA1* and *LHY*. We find that even in optimal growth conditions, these new quintuple mutants are only marginally rhythmic, with very low-amplitude rhythms. However, these plants have hypocotyl and rosette growth phenotypes comparable with wild-type plants, similar to the previously described phenotypes of the partial loss-of-function quintuple mutants (Shalit-Kaneh et al., 2018). We also used the new quintuple mutant to analyze epistasis because partial loss-of-function alleles are unreliable when assessing epistatic interactions (Avery & Wasserman, 1992). We suggest that these activating and repressing core clock Myb-like factors interact epistatically in the control of circadian rhythms and flowering time, but additively in the control of several growth phenotypes. Our results emphasize that phenotypes observed in plants mutant for core circadian clock genes are not always due to changes in rhythmicity per se but may be due to altered regulation of downstream processes by core clock transcription factors.

2 | RESULTS

2.1 | *CCA1* and *LHY* are epistatic to *RVE4*, *RVE6*, and *RVE8* for circadian clock and flowering time function

We generated a new *cca1 lhy rve468* mutant containing *lhy-100* (Martin-Tryon et al., 2007), a nonsense mutation, rather than the hypomorphic *lhy-20* allele (Michael et al., 2003). We also used CRISPR-Cas9 to create new frameshift mutations in *RVE4*, *RVE6*, and *RVE8*, all of which are predicted to cause premature stop codons and loss of function (Figure 1a, Figure S1). In *RVE4*, this frameshift occurred in the first exon, upstream of the Myb-like DNA-binding domain (Figures 1a and S1). In *RVE6*, this frameshift occurred in the third exon, within the conserved proline-rich region just downstream of the Myb-like domain (Figures 1a and S1). In *RVE8*, this frameshift occurred in the fourth exon, upstream of the conserved C-terminal domain (Figures 1a and S1). The Cas9-negative *cca1-1 lhy-100 rve4-12 rve6-12 rve8-12* (hereafter referred to as *cca1 lhy rve468-12*) line generated from these new alleles is likely a null mutant.

To investigate the rhythmicity of *cca1 lhy rve468-12*, we monitored circadian regulation of expression of a clock-regulated reporter gene, *CCR2::LUC2*, in a range of light qualities, light intensities, and temperatures. Rhythmicity of *cca1 lhy rve468-12* was compared with wild-type Col-0, *rve4-11 rve6-11 rve8-11* (Figure S1) and *cca1-1 lhy-100* (hereafter referred to as *cca1 lhy*). The *rve4-11 rve6-11 rve8-11* alleles (hereafter referred to as *rve468-11*) were generated using the same guide RNAs as the *rve4-12 rve6-12 rve8-12* alleles and have frameshift mutations in nearly identical locations. These are also predicted to cause premature stop codons and loss of function (Figure S1, Data S1). In constant darkness and the standard growth temperature of 22°C, both Col-0 and *rve468-11* are robustly rhythmic while *cca1 lhy* and *cca1 lhy rve468-12* have generally poor rhythms with less than 25% of plants defined as rhythmic (Figure 1b). Across a range of light intensities (from 1 to 200 µmol m^{-2} s^{-1}) of constant red plus blue, monochromatic red, or monochromatic blue light, Col-0 and

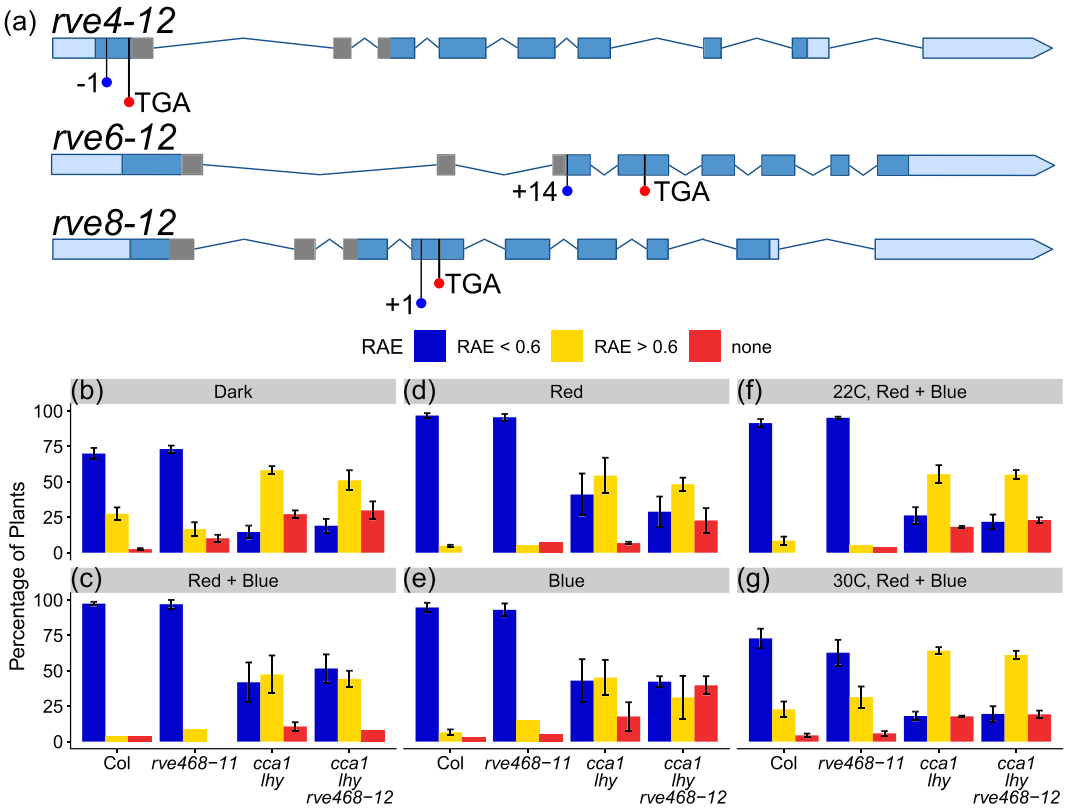

FIGURE 1 *cca1 lhy rve468-12* mutants have poor rhythms in all conditions tested. (a) Gene models of CRISPR-Cas9-generated *rve4-12*, *rve6-12*, and *rve8-12* alleles. Positions of insertions or deletions are shown by blue circles and positions of resulting premature stop codons are shown by red circles. Light blue represents untranslated regions while dark blue represents coding regions. Gray shading represents the coding regions of the Myb-like DNA-binding domains. (b–g) Rhythmicity as measured by relative amplitude error (RAE) across light qualities and temperatures, where RAE < 0.6 is defined as rhythmic and RAE > 0.6 defined as arrhythmic. Seedlings with luciferase activity that could not be fit to any cosine curve did not return an RAE. (b) After entrainment at 22°C, seedlings were transferred to constant darkness at 22°C. Data from three biological replicates, $n = 33–106$ per replicate. (c–e) After entrainment at 22°C, seedlings were transferred to constant 10 µmol m^{-2} s^{-1} light of the specified quality at 22°C. Data from three biological replicates, $n = 11–36$ per replicate. (f, g) After entrainment at 22°C, seedlings were transferred to 35 µmol m^{-2} s^{-1} red plus 35 µmol m^{-2} s^{-1} blue light at the specified temperature. Data from two biological replicates, $n = 34–71$ per replicate.

rve468-11 are similarly and highly rhythmic while *cca1 lhy* and *cca1 lhy rve468-12* both exhibit dampened rhythms (Figures 1c–f and S2). This pattern is also observed at 30°C, where *cca1 lhy* and *cca1 lhy rve468-12* have similarly dampened rhythms while Col-0 and *rve468-11* exhibit robust rhythms (Figure 1g). In all tested conditions except 100 µmol m^{-2} s^{-1} monochromatic red and 100 µmol m^{-2} s^{-1} red plus blue light, the proportion of rhythmic plants in *cca1 lhy* and *cca1 lhy rve468-12* was not significantly different from each other but was significantly different from Col-0 (Figure S2; Pearson's chi-squared and pairwise proportion test with Benjamin–Hochberg correction; $p < 0.05$). These data indicate that *cca1 lhy* and *cca1 lhy rve468-12* have similarly poor rhythmicity across a range of growth conditions.

To further compare the circadian phenotypes of *cca1 lhy* and *cca1 lhy rve468-12*, we examined the circadian periods of the small fraction of plants of these genotypes considered rhythmic (relative amplitude error (RAE) < 0.6) in different light qualities. In constant darkness, 10 µmol m^{-2} s^{-1} red plus blue, and 10 µmol m^{-2} s^{-1} monochromatic blue light, the periods of *cca1 lhy* and *cca1 lhy rve468-12* seedlings are significantly different from those of *rve468-11* seedlings but not significantly different from each other (Figure S3). In 10 µmol m^{-2} s^{-1} monochromatic red light, *cca1 lhy rve468-12* has a significantly longer period than *cca1 lhy* but is still considerably shorter than *rve468-11* (Figure S3). Together, these data indicate that *cca1 lhy rve468-12* has similar circadian phenotypes to *cca1 lhy*.

Based on the dampened rhythms of *cca1 lhy rve468-12* mutants, we hypothesized that rhythmic oscillator function would be quickly lost in free-running conditions. To assess the expression patterns of core clock genes in these mutants, we next extracted RNA from plants grown in constant white light and carried out quantitative reverse-transcriptase polymerase chain reaction (qRT-PCR) assays. Expression of *PRR5*, *TOC1*, *ELF4*, and *LUX* is rhythmic in Col-0 and *rve468-11*, but the amplitude of rhythmic expression is severely reduced in *cca1 lhy* and *cca1 lhy rve468-12* (Figure 2), as expected based on our luciferase data (Figures 1 and S2). Mean expression of *LUX* and *PRR5* over the entire time course is significantly higher in both *cca1 lhy* and *cca1 lhy rve468-12* compared with wild type (one-way ANOVA and Tukey's post hoc test, $p < 1e^{-3}$). While mean expression of *TOC1* and *ELF4* across the time course is not significantly different in *cca1 lhy* and *cca1 lhy rve468-12* compared with Col-0, in both cases these transcripts are dampening towards the peak levels of expression in wild type (Figure 2). For all clock genes examined, mean expression values are not significantly different between *cca1 lhy* and *cca1 lhy rve468-12* across the examined time points (one-way ANOVA and Tukey's post hoc test, $p > 0.05$). These data suggest that in constant conditions the loss of the repressive activity of CCA1 and LHY is epistatic to the loss of the activating function of the RVE proteins for these central clock genes.

We next examined expression of a clock-regulated reporter gene, *CCR2::LUC2*, in *cca1 lhy rve468-12* and the parental mutants maintained in light–dark cycles to determine expression patterns in the presence of environmental cues. In seedlings subjected to long day (LD) photoperiods (16 h light, 8 h dark), the waveforms of *cca1 lhy rve468-12* are very similar to those of *cca1 lhy* but different from Col-0 and *rve468-11* (Figures 3 and S4). Notably, both *cca1 lhy* and *cca1 lhy rve468-12* exhibit a sharp increase in luciferase activity shortly after dawn, suggesting decreased circadian regulation and increased responsiveness to environmental cues in these genotypes. In short day (SD) photoperiods (8 h light, 16 h dark), a similar pattern was observed in both *cca1 lhy* and *cca1 lhy rve468-12* (Figures 3 and S4). This suggests that circadian function is similarly disrupted in *cca1 lhy* and *cca1 lhy rve468-12* mutants.

To further investigate the relationship between *CCA1*, *LHY*, *RVE4*, *RVE6*, and *RVE8*, we next examined the photoperiodic regulation of

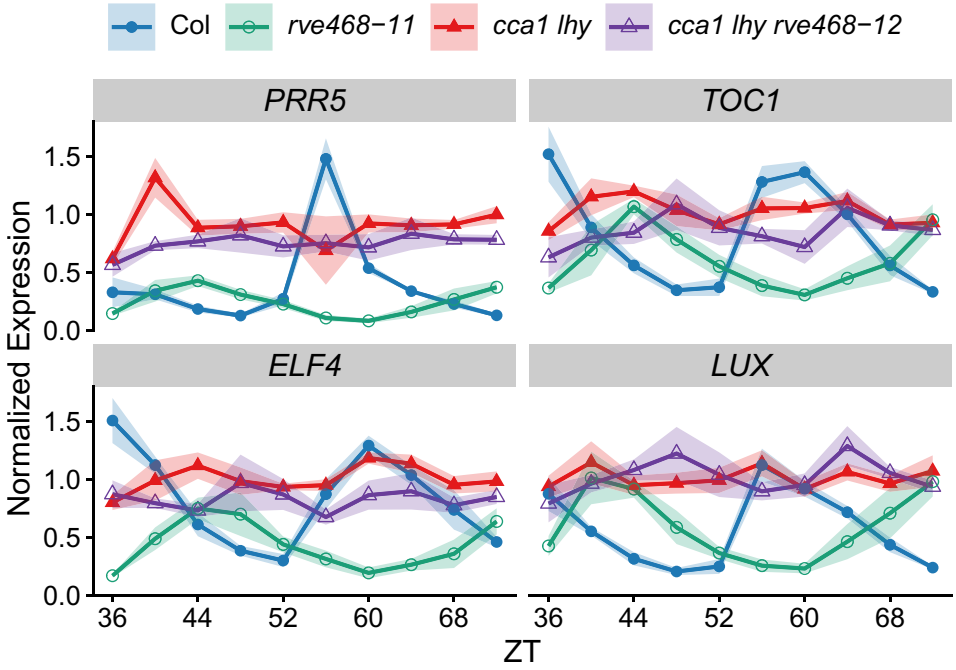

FIGURE 2 Rhythmicity of core clock gene expression is severely reduced in *cca1 lhy* and *cca1 lhy rve468-12* mutants. After entrainment, seedlings were transferred at ZT0 to constant 50–60 µmol m^{-2} s^{-1} white light at 22°C. Expression of the specified genes was determined by qRT-PCR and normalized to reference genes *PP2A* and *IPP2*. Ribbon indicates ± SEM for four biological replicates.

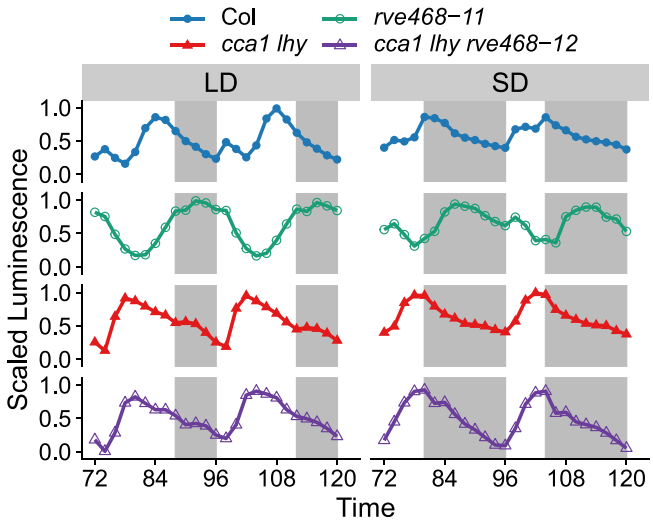

FIGURE 3 Diel waveforms of gene expression in *cca1 lhy* and *cca1 lhy rve468-12* mutants are similar to each other. Average traces of luminescence from *CCR2::LUC2* transgene in the indicated genotypes. Gray boxes show periods of darkness. Seedlings were entrained in 12:12 light–dark cycles, then transferred at time 0 to 12:12 light–dark cycles with 35 μmol m^{-2} s^{-1} red plus 35 μmol m^{-2} s^{-1} blue light at 22°C. At time 48, light–dark cycles were changed to either 16:8 (LD) or 8:16 (SD) under the same light intensities. $N = 16–18$, experiment was conducted twice with similar results. The full time course is presented in Figure S4.

the transition from vegetative to reproductive growth as this response depends upon a functional circadian system (Maeda & Nakamichi, 2022; Song et al., 2015). In long days, *rve468-11* flowers significantly later than Col-0 when measured either by leaf number or days (Figure 4), as previously observed (Gray et al., 2017). In contrast, both *cca1 lhy* and *cca1 lhy rve468-12* flower significantly earlier than Col-0 in long days when measured by leaf number (Figure 4). In short days, *rve468-11* flowers significantly later than Col-0 when measured by days but not when measured by leaf number (Figure 4). As in long days, *cca1 lhy* and *cca1 lhy rve468-12* both flower significantly earlier than Col-0 in short days when measured either by leaf number or days. While *cca1 lhy rve468-12* flowers significantly later than *cca1 lhy* in short days, the flowering time is much closer to that of *cca1 lhy* than to *rve468-11* (Figure 4). Overall, in both long and short days, flowering time for the *cca1 lhy rve468-12* mutant is similarly early as for *cca1 lhy*. Together, the gene expression and flowering time data suggest that *CCA1* and *LHY* are epistatic to *RVE4*, *RVE6*, and *RVE8* in circadian clock function and its coordination of flowering time.

2.2 | *CCA1*, *LHY*, *RVE4*, *RVE6*, and *RVE8* are additive for growth

Given the similar circadian phenotypes of *cca1 lhy* and *cca1 lhy rve468-12*, we next wanted to compare the growth phenotypes of *cca1 lhy rve468-12* and *cca1 lhy*. As hypocotyl elongation is regulated by the circadian clock (Dowson-Day & Millar, 1999), we hypothesized that *cca1 lhy rve468-12* mutants would have short hypocotyls like *cca1 lhy* mutants. We grew seedlings in constant darkness or in constant light with intensities ranging from 0.1 to 30 μmol m^{-2} s^{-1} for 6 days and then measured their hypocotyl lengths. In all constant light conditions (monochromatic red, monochromatic blue, and red plus blue), *cca1 lhy* hypocotyls are shorter and *rve468-11* hypocotyls are longer than Col-0 (Figure 5), consistent with previous reports (Gray et al., 2017; Hall et al., 2003; Más et al., 2003). Interestingly, *cca1 lhy rve468-12* has an intermediate hypocotyl length that is not significantly different from Col-0 in most light conditions (one-way ANOVA and Tukey's post hoc test, $p > 0.05$) (Figure 5). These data suggest that *CCA1*, *LHY*, *RVE4*, *RVE6*, and *RVE8* interact additively to regulate hypocotyl length in constant light conditions.

We next examined genetic interactions between *CCA1*, *LHY*, *RVE4*, *RVE6*, and *RVE8* on phenotypes of adult plants, measuring the petiole length and blade area of the fully expanded fifth rosette leaf of plants grown in long or short photoperiods. The overall appearance of *cca1 lhy rve468-12* plants is intermediate between that of the *cca1 lhy* and *rve468-11* mutants in both LD and SD conditions (Figure 6a,b). In short days, *rve468-11* has a significantly longer median petiole length than Col-0, and *cca1 lhy* has a significantly shorter median petiole length than Col-0 (Figure 6c), consistent with previous observations (Gray et al., 2017). However, the median petiole length of *cca1 lhy rve468-12* is intermediate between that of *cca1 lhy* and Col-0 in both photoperiods (Figure 6c), suggesting an additive genetic interaction between the positive and negative-acting Myb-like factors. The median blade area of *cca1 lhy* is significantly smaller than Col-0 in both long days and short days. Surprisingly, *rve468-11* has a significantly larger median blade area than Col-0 in long days, consistent with previous observations (Gray et al., 2017), but a significantly smaller median blade area than Col-0 in short days (Figure 6c). The median blade area of *cca1 lhy rve468-12* is larger than *cca1 lhy* in both photoperiods, although this does not reach statistical significance in long days, likely due to a high degree of variation in this condition (Figure 6c). Together, these data suggest that *CCA1*, *LHY*, *RVE4*, *RVE6*, and *RVE8* interact additively to regulate elongation of hypocotyls in constant light and growth of leaves in long and short days.

2.3 | Loss of the *RVE*s does not rescue *PIF4* and *PIF5* expression in *cca1 lhy* mutants

PIF4 and *PIF5* are required for the large rosette size of *rve468* mutants and their expression is significantly increased in *rve468* (Gray et al., 2017). We therefore hypothesized that expression of these genes might be elevated in *cca1 lhy rve468-12* compared with *cca1 lhy* and that this might contribute to their differences in size. We therefore examined *PIF* expression under constant white light using qRT-PCR. As expected based on the expression patterns of the core clock genes (Figure 2), *PIF4* and *PIF5* expression is poorly rhythmic in both *cca1 lhy* and in *cca1 lhy rve468-12* (Figure 7). To our surprise, however, we found that expression levels of *PIF4* and *PIF5* in the double *cca1 lhy* and the quintuple *cca1 lhy rve468-12* plants are similarly

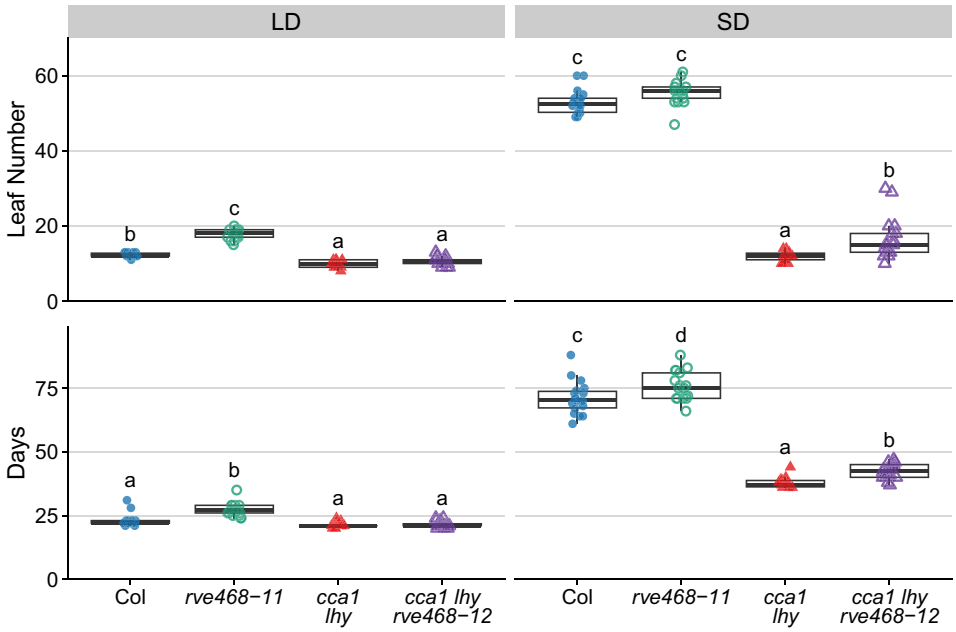

FIGURE 4 *CCA1* and *LHY* are epistatic to *RVE4*, *RVE6*, and *RVE8* for flowering time regulation. Flowering time of the indicated genotypes was assessed by leaf number at bolting and days to bolting. Bolting was defined as the time when the inflorescence stem reached 1 cm. Plants were grown at 22°C under 150–200 μmol m^{-2} s^{-1} white light in the specified photoperiods (16:8 LD or 8:16 SD). Different letters denote significant differences between genotypes within each condition ($p < 0.01$), determined by one-way ANOVA followed by Tukey's post hoc test. The lines within the boxes are the medians, and the lower and upper hinges represent the first and third quartiles. $N = 14–18$, experiment was conducted twice with similar results. Mean values and results of all statistical comparisons may be found in Data S4.

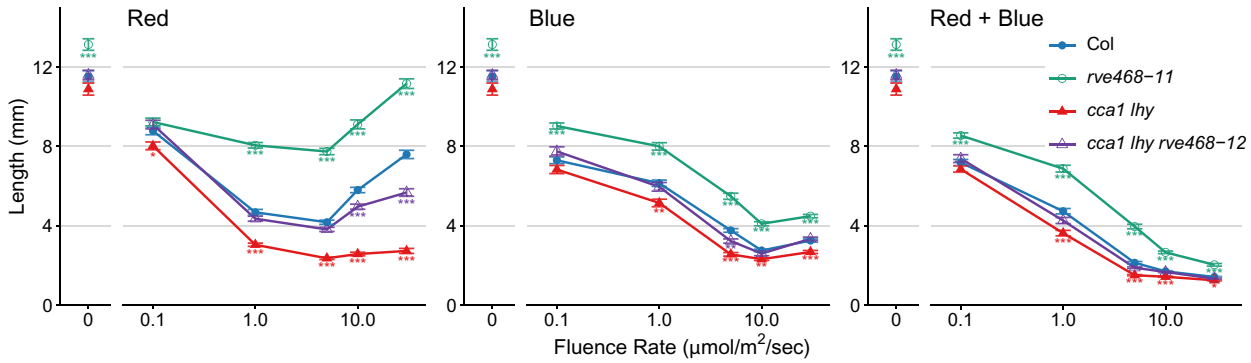

FIGURE 5 *CCA1*, *LHY*, *RVE4*, *RVE6*, and *RVE8* interact additively to regulate hypocotyl length. Hypocotyl length of the indicated genotypes was determined in different light qualities and intensities. Seedlings were grown at 22°C under constant darkness or monochromatic red, monochromatic blue, or red plus blue light of the specified intensity (0.1–30 μmol m^{-2} s^{-1}). Mean hypocotyl length is shown, error bars indicate ± SEM. Significant differences between genotypes in each light quality and fluence rate determined by one-way ANOVA followed by Tukey's post hoc test (*$p < 0.05$, **$p < 0.01$, ***$p < 0.001$). Only comparisons between each genotype and Col-0 are shown. In constant light conditions, data from three biological replicates ($n = 15–22$ per replicate). In constant darkness, data from six biological replicates ($n = 7–21$ per replicate). Mean values and results of all statistical comparisons may be found in Data S4.

low and not significantly different between these two genotypes (one-way ANOVA and Tukey's post hoc test, $p > 0.05$). Because other clock proteins are known to modulate PIF transcriptional regulatory activity (Martín et al., 2018; Soy et al., 2016; Zhang et al., 2020), we next hypothesized that there might be differences in PIF4 and/or PIF5 activity in *cca1 lhy* and *cca1 lhy rve468-12* mutants. We therefore examined expression levels of known *PIF4* and *PIF5* targets implicated in auxin signaling and hypocotyl elongation, including *TRYPTOPHAN AMINOTRANSFERASE OF ARABIDOPSIS 1* (*TAA1*), *INDOLE-3-ACETIC ACID INDUCIBLE 29* (*IAA29*), *YUCCA 8* (*YUC8*), and *ARABIDOPSIS THALIANA HOMEOBOX PROTEIN 2* (*ATHB2*) (Franklin et al., 2011; Koini et al., 2009; Kunihiro et al., 2011; Nozue et al., 2011; Steindler et al., 1999; Sun et al., 2012; Tao et al., 2008). Like the expression of *PIF4* and *PIF5* themselves, the overall expression patterns and mean levels of these genes are similar between *cca1 lhy* and *cca1 lhy rve468-12*, although mean expression levels of *TAA1*

FIGURE 6 *CCA1*, *LHY*, *RVE4*, *RVE6*, and *RVE8* interact additively to regulate leaf growth. (a) Representative images of plants grown for 35 days in 16:8 light–dark cycles (LD) at 22°C. (b) Representative images of plants grown for 35 days in 8:16 light–dark cycles (SD) at 22°C. (c) Petiole length and blade area of rosette leaf 5 of the indicated genotypes were assessed after 30 days of growth in the specified photoperiods. Different letters denote significant differences between genotypes within each condition ($p < 0.01$), determined by one-way ANOVA followed by Tukey's post hoc test. The lines within the boxes are the medians, and the lower and upper hinges represent the first and third quartiles. $N = 17–18$, experiment was conducted twice with similar results. Plants were grown at 22°C under 150–200 µmol m^{-2} s^{-1} white light (a–c). Mean values and results of all statistical comparisons may be found in Data S4.

and *ATHB2* over the entire time course are slightly but significantly higher in *cca1 lhy* than in *cca1 lhy rve468-12* (one-way ANOVA and Tukey's post hoc test, $p < 0.05$) (Figure 7). These data suggest that expression differences of *PIF4*, *PIF5*, and at least several of their targets involved in auxin biosynthesis or signaling are likely not responsible for observed differences in growth between *cca1 lhy* and *cca1 lhy rve468-12*.

3 | DISCUSSION

Here, we present a likely null *cca1 lhy rve468* quintuple mutant and examine its clock and growth phenotypes compared with *cca1 lhy* and *rve468* mutants. We find that *CCA1* and *LHY* are epistatic to *RVE4*, *RVE6*, and *RVE8* in the regulation of the circadian clock and flowering time. However, *CCA1* and *LHY* are additive to *RVE4*, *RVE6*, and *RVE8* in the regulation of growth phenotypes. Interestingly, *cca1 lhy rve468-12* quintuple mutants grow similarly to wild-type plants despite being largely arrhythmic, suggesting that a functional oscillator is not required for near-normal phenotypes of circadian-regulated outputs.

3.1 | Mutants with T-DNAs integrated into introns can be unstable

There are conflicting reports in the literature regarding the overall rhythmicity of *cca1 lhy* mutants. In the Col-0 background, the *cca1-1* and *lhy-20* alleles are both T-DNA insertion mutants (Green & Tobin, 1999; Michael et al., 2003), and the double mutant has been described as either arrhythmic or rhythmic with a short-period phenotype (Marshall et al., 2016; Shalit-Kaneh et al., 2018; Yakir et al., 2009; Yuan et al., 2021; Zhang et al., 2013). A similar trend is observed with the *cca1-11 lhy-21* mutant in the Wassilewskija (Ws) background, which has been reported to be either arrhythmic or rhythmic with a short-period phenotype (Hall et al., 2003; Locke et al., 2005; Lu et al., 2009). Some of these differences in reported rhythmicity may well be attributed to differences in growth conditions and the types of assays used to assess rhythmicity. However, we propose that some of these reported phenotypic differences may be due to instability of mutant alleles in which a T-DNA insertion has occurred within a non-coding portion of the gene (as is true for *cca1-1*, *cca1-11*, and *lhy-20*).

There are multiple reports of T-DNA suppression of the phenotypes of mutants with a T-DNA insertion within an intron (Gao & Zhao, 2013; Osabe et al., 2017; Sandhu et al., 2013; Xue et al., 2012). This phenomenon is analogous to paramutation in that introduction of a second T-DNA locus induces the genetically stable upregulated expression of a previously silenced locus. The mechanism depends upon the RNA-dependent DNA methylation pathway and hypermethylation of intronic T-DNA sequences in the suppressed allele (Osabe et al., 2017; Sandhu et al., 2013; Xue et al., 2012). This process may have caused partial suppression of the *lhy-20* allele in the *cca1-1*

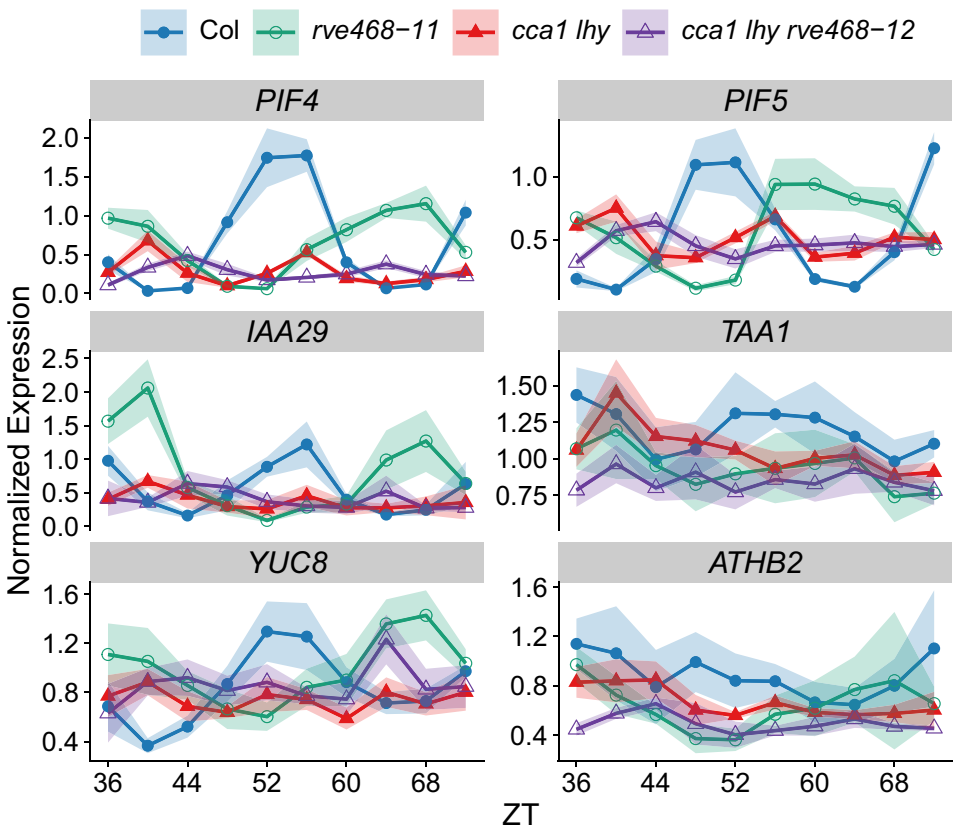

FIGURE 7 Expression of *PIF4*, *PIF5*, and PIF target genes is low and arrhythmic in *cca1 lhy* and *cca1 lhy rve468-12* mutants. After entrainment, seedlings were transferred at ZT0 to constant 50–60 μmol m^{-2} s^{-1} white light at 22°C. Expression of the specified genes was determined by qRT-PCR and normalized to reference genes *PP2A* and *IPP2*. Ribbon indicates ± SEM for four biological replicates.

lhy-20 double mutant as we observe considerable *LHY* expression in these plants (Shalit-Kaneh et al., 2018).

In the *cca1-1 lhy-20 rve4-1 rve6-1 rve8-1* mutant, all alleles contain homologous T-DNA sequences inserted within introns that could potentially allow T-DNA suppression to occur. This possibility is supported by our observation that although we did not detect *RVE4* or *RVE8* expression when we first isolated the *rve4-1 rve6-1 rve8-1* mutants (Hsu et al., 2013; Shalit-Kaneh et al., 2018), after further generations of propagation, we now detect considerable expression of *RVE4* and *RVE8* in these plants (Figure S5). We therefore expect that the new CRISPR-edited frameshift mutants of *RVE4*, *RVE6*, and *RVE8* that we report in this paper will, as stable alleles, prove very useful to the plant science community.

3.2 | Improper circadian regulation does not guarantee altered growth phenotypes

Mutant circadian phenotypes are often correlated with abnormal growth phenotypes, such as *rve468* mutants having a long period (Hsu et al., 2013) as well as long hypocotyls and large rosettes (Gray et al., 2017). Often such phenotypes are attributed to the malfunctioning of the circadian clockwork. However, most clock components are connected to many other pathways, such as the regulation of growth through control of *PIF4* and *PIF5* expression by the evening complex (Nusinow et al., 2011). Many clock proteins are not only components of the circadian clock itself but also transcription factors that can directly control expression of hundreds of clock-controlled genes. This makes it difficult to determine if mutant phenotypes are due to disrupted clock function or due to altered expression levels of clock output genes. Here, we show that *cca1 lhy rve468-12* is a mutant with highly reduced clock function but with similar hypocotyl (Figure 5) and rosette growth phenotypes (Figure 6) as wild-type plants. Especially in the constant-light conditions frequently used to assess hypocotyl elongation, these data show that robust rhythmicity per se is not required for near-normal growth responses.

3.3 | Plants mutant for all five Myb-like factors are photoperiodic

Although rhythmicity of free-running gene expression is greatly reduced in *cca1 lhy rve468-12* mutants (Figures 1 and 2), these plants retain photoperiodic responsiveness. The quintuple mutants flower later in short days than in long days as measured either by days to flowering or number of leaves produced before flowering (one-way ANOVA, $p < 1e^{-10}$ for both comparisons) (Figure 4; Data S1). This suggests that some clock function is retained even in these quintuple mutants. This is supported by our detection of some rhythmic *cca1 lhy rve468-12* plants in luciferase assays (Figures 1 and S2). This is most noticeable in constant red plus blue light conditions, where up to half of the *cca1 lhy rve468-12* seedlings had an RAE < 0.6 in at least one experiment (Figure S2). qRT-PCR analysis also suggested some

genes, like *LUX*, may have low-amplitude rhythms of gene expression in the quintuple mutant in constant conditions (Figure 2).

It is surprising that *cca1 lhy rve468-12* retains some level of clock function given that these five core clock genes are involved in the main feedback loops within the core circadian clock (Creux & Harmer, 2019; Davis et al., 2022). However, two homologous Myb-like proteins, RVE3 and RVE5, have been previously shown to play a very modest role in the circadian system (Gray et al., 2017). It is therefore possible that these factors may partially compensate for the five genes mutated in *cca1 lhy rve468-12* plants. It is also possible that the transcriptional feedback loops involving the Myb-like factors are not essential for all circadian function. For example, it known that the evening complex can regulate itself, with *LUX* binding to its own promoter (Helfer et al., 2011) and that the evening complex and PRRs reciprocally repress each other's expression (Dixon et al., 2011; Helfer et al., 2011; Huang et al., 2012). It may be that these feedback loops are sufficient on their own to sustain the slight circadian function observed in plants mutant for the five Myb-like proteins. In this scenario, additional feedback loops involving the Myb-like proteins would allow the clock to better synchronize with the environment and cycle more robustly but would not be necessary for a low level of basal rhythmicity.

4 | MATERIALS AND METHODS

4.1 | Plant materials

All plants used are in the Columbia (Col-0) wild-type background. The *cca1-1* allele originally in the Wassilewskija (Ws) background (Green & Tobin, 1999) was backcrossed to Col-0 for six generations, then crossed to *lhy-100*[46] to generate *cca1-1 lhy-100*. This mutant was then transformed via floral dip (Clough & Bent, 1998) with the pC2L2 construct containing *CCR2::LUC2* to generate the *cca1-1 lhy-100 CCR2::LUC2* line used here. Col *CCR2::LUC2* was generated by crossing *cca1-1 lhy-100 CCR2::LUC2* to Col-0 and isolating plants without mutations in *cca1* or *lhy*. The *rve4-11 rve6-11 rve8-11 CCR2::LUC2* mutant was generated by transforming Col *CCR2::LUC2* with the 8X-*RVE*_pMR333 Cas9-containing construct via floral dip (Clough & Bent, 1998). The *cca1-1 lhy-100 rve4-12 rve6-12 rve8-12 CCR2::LUC2* mutant was generated by transforming *cca1-1 lhy-100 CCR2::LUC2* with the 8X-*RVE*_pMR333 Cas9-containing construct via floral dip (Clough & Bent, 1998). Transgenic plants were initially selected on media containing 30 mg/L Basta and Cas9-negative lines were later selected for study. For Figure S5, Col *CCR2::LUC+*, *rve4-1 CCR2::LUC+*, *rve8-1 CCR2::LUC+*, and *rve4-1 rve6-1 rve8-1 CCR2::LUC+* are as previously described (Hsu et al., 2013; Rawat et al., 2011).

4.2 | Plasmids

The pC2L2 plasmid was created through traditional cloning methods by replacing *LUC+* within the previously described *CCR2::LUC+* plasmid (Strayer et al., 2000) with *LUC2* from pGL4.10 (Promega, Madison, WI). The 8X-*RVE*_pMR333 plasmid was created through Gateway cloning (Hartley et al., 2000) between 8X-*RVE*_pEn-Chimera and pMR333 (generously donated by Dr. Mily Ron). CRISPR-Cas9 guides targeting *RVE3*, *RVE4*, *RVE6*, and *RVE8* were designed using the CRISPOR algorithm (Concordet & Haeussler, 2018; Haeussler et al., 2016), multiplexed by interspersing tRNA and gRNA sequences as previously described (Xie et al., 2015), and synthesized by Genewiz (Genewiz, South Plainfield, NJ). Guide sequences are included in Data S2. The synthesized guide fragment was incorporated into pEn-Chimera (Fauser et al., 2014) through traditional cloning methods to create 8X-*RVE*_pEn-Chimera.

4.3 | Genotyping

New CRISPR-Cas9 alleles were identified through PCR amplification followed by Sanger sequencing, mutant sequences included in Data S1. Homozygous mutants of all alleles used in this research were identified through PCR amplification of genomic DNA. Primers used for genotyping are included in Data S3.

4.4 | Growth conditions

Seeds were surface sterilized with chlorine gas and stratified in the dark for 2–4 days at 4°C. For luciferase imaging and qRT-PCR, seeds were plated on 1× Murashige and Skoog, .7% agar, 3% sucrose. Seedlings were entrained in light–dark cycles (12 h light, 12 h dark) under 50–60 μmol m^{-2} s^{-1} white light at 22°C for 6 days. For hypocotyl length assays, seeds were plated on 0.5X Murashige and Skoog, .7% agar and exposed to a 4-h pulse of 50–60 μmol m^{-2} s^{-1} white light at 22°C to induce germination. Seedlings were then grown in the specified light conditions using monochromatic red and/or blue LEDs (XtremeLUX, Santa Clara, CA) at 22°C for 6 days. For flowering time and rosette growth assays, seeds were sown directly on soil and grown in light–dark cycles of the specified photoperiod under 150–200 μmol m^{-2} s^{-1} white light at 22°C.

4.5 | *CCR2::LUC2* luciferase imaging

Seedlings were sprayed with 3 mM D-luciferin, moved to the specified light conditions using red and/or blue LEDs (XtremeLUX, Santa Clara, CA), and imaged for 5–6 days under a cooled CCD camera (DU434-BV, Andor Technology, or iKon M-934, Andor Technology). Neutral density filters (Rosco Laboratories or LEE Filters) were used to generate the specified light intensities of monochromatic red, monochromatic blue, or red plus blue light (Figures 1c–e, S2, and S3). Quantification of bioluminescence was performed using MetaMorph software (Molecular Devices), and circadian rhythms were analyzed with Biological Rhythm Analysis Software System (BRASS) (Locke et al., 2005).

4.6 | Calculating scaled luminescence

For Figures 3 and S4, luminescence values of all individual plants were averaged for each genotype at each time point. Background luminescence was then removed across the experiment so that trough values were close to 0. Finally, these luminescence values were scaled so that maximum luminescence across the time series was set to 1 for each genotype.

4.7 | qRT-PCR analysis

After entrainment, seedlings were moved to constant 50–60 µmol m^{-2} s^{-1} white light at 22°C at dawn (ZT0) and collected every 4 h from ZT36 to ZT72. Sample preparation and qRT-PCR were performed as previously described (Shalit-Kaneh et al., 2018) using a BioRad CFX96 thermocycler (Bio-Rad Laboratories, Hercules, CA). Relative expression and SEM values were obtained from the BioRad CFX96 software package. Primers used for qRT-PCR are included in Data S3.

4.8 | Hypocotyl length assays

After 6 days of growth, seedlings were transferred to transparent sheets and scanned at 600 dpi. Hypocotyls were individually measured using ImageJ (Schneider et al., 2012).

4.9 | Flowering time analysis

Date of flowering was recorded as the day the inflorescence stem reached 1 cm long. At that time, rosette leaves were counted to determine flowering time by leaf number. Cauline leaves were not included.

4.10 | Rosette leaf measurements

After 30 days of growth, rosette leaf 5 was transferred to transparent sheets and scanned at 600 dpi. Blade area and petiole length were measured using LeafJ (Maloof et al., 2013).

4.11 | Statistical analysis and data visualization

All statistical analyses and data visualization were performed using R (R Core Team, 2023). Figures were generated using the tidyverse (Wickham et al., 2019), RColorBrewer (Neuwirth, 2022), cowplot (Wilke, 2020), gridExtra (Auguie, 2017), glue (Hester & Bryan, 2022), and ggtext (Wilke, 2022) packages. Gene models were created using the genemodel package (Monroe, 2017). Statistical differences in fractions of rhythmic plants between genotypes were determined by Pearson's chi-squared test, followed by pairwise proportion tests with Benjamin–Hochberg correction for multiple testing using the rstatix package (Kassambara, 2021). Linear mixed-effect models were used in one-way ANOVA and Tukey's post hoc tests to compare mean expression level between genotypes for qRT-PCR analysis, period phenotype differences between genotypes, flowering time and rosette growth differences between genotypes within each condition (LD or SD), and hypocotyl length differences between genotypes at each fluence rate. Modeling was done with the lme4 (Bates et al., 2015) and lmerTest (Kuznetsova et al., 2017) packages, tests were performed using the lattice (Sarkar, 2008), broom (Robinson et al., 2023), and emmeans (Lenth, 2021) packages. Results were visualized with the multcomp (Hothorn et al., 2008) and multcompView (Graves et al., 2019) packages.

4.12 | Accession numbers

Accession numbers for *A. thaliana* genes referenced here:

ATHB2 - AT4G16780.
CCA1 - AT4G16780.
CO - AT5G15840.
ELF3 - AT2G25930.
ELF4 - AT2G40080.
FT - AT1G65480.
IAA29 - AT1G65480.
LHY - AT1G01060.
LUX - AT3G46640.
PIF4 - AT2G43010.
PIF5 - AT3G59060.
PRR5 - AT3G59060.
PRR7 - AT5G02810.
PRR9 - AT2G46790.
RVE4 - AT5G02840.
RVE6 - AT5G52660.
RVE8 - AT3G09600.
TAA1 - AT1G70560.
TOC1 - AT5G61380.
YUC8 - AT4G28720.

AUTHOR CONTRIBUTIONS

Cassandra L. Hughes and Stacey L. Harmer designed the project. Cassandra L. Hughes performed the research. Cassandra L. Hughes and Stacey L. Harmer analyzed data and wrote the manuscript.

ACKNOWLEDGMENTS

This work was supported by an award from the National Institutes of Health (R01 GM069418) and the US Department of Agriculture-National Institute of Food and Agriculture (CA-D-PLB-2259-H). We thank Julin Maloof for advice on statistical issues and members of the Harmer lab for many helpful discussions.

CONFLICT OF INTEREST STATEMENT

The authors declare no conflict of interest associated with the work described in this manuscript.

PEER REVIEW

The peer review history for this article is available in the Supporting Information for this article.

DATA AVAILABILITY STATEMENT

The data that support the findings of this study are available from the corresponding author upon reasonable request.

ORCID

Cassandra L. Hughes https://orcid.org/0009-0004-7001-3250

Stacey L. Harmer https://orcid.org/0000-0001-6813-6682

REFERENCES

Adams, S., Grundy, J., Veflingstad, S. R., Dyer, N. P., Hannah, M. A., Ott, S., & Carré, I. A. (2018). Circadian control of abscisic acid biosynthesis and signalling pathways revealed by genome-wide analysis of LHY binding targets. *The New Phytologist*, *220*(3), 893–907. https://doi.org/10.1111/nph.15415

Alabadí, D., Oyama, T., Yanovsky, M. J., Harmon, F. G., Más, P., & Kay, S. A. (2001). Reciprocal regulation between TOC1 and LHY/CCA1 within the Arabidopsis circadian clock. *Science*, *293*(5531), 880–883. https://doi.org/10.1126/science.1061320

Alabadí, D., Yanovsky, M. J., Más, P., Harmer, S. L., & Kay, S. A. (2002). Critical role for CCA1 and LHY in maintaining circadian rhythmicity in Arabidopsis. *Current Biology*, *12*(9), 757–761. https://doi.org/10.1016/S0960-9822(02)00815-1

Auguie, B. (2017). *gridExtra: Miscellaneous functions for "Grid" graphics*. https://CRAN.R-project.org/package=gridExtra

Avery, L., & Wasserman, S. (1992). Ordering gene function: The interpretation of epistasis in regulatory hierarchies. *Trends in Genetics*, *8*(9), 312–316. https://doi.org/10.1016/0168-9525(92)90263-4

Bates, D., Mächler, M., Bolker, B., & Walker, S. (2015). Fitting linear mixed-effects models using lme4. *Journal of Statistical Software*, *67*(1), 1–48. https://doi.org/10.18637/jss.v067.i01

Clough, S. J., & Bent, A. F. (1998). Floral dip: A simplified method for agrobacterium-mediated transformation of *Arabidopsis thaliana*. *The Plant Journal*, *16*(6), 735–743. https://doi.org/10.1046/j.1365-313x.1998.00343.x

Concordet, J. P., & Haeussler, M. (2018). CRISPOR: Intuitive guide selection for CRISPR/Cas9 genome editing experiments and screens. *Nucleic Acids Research*, *46*(W1), W242–W245. https://doi.org/10.1093/nar/gky354

Creux, N., & Harmer, S. (2019). Circadian rhythms in plants. *Cold Spring Harbor Perspectives in Biology*, *11*(9), a034611. https://doi.org/10.1101/cshperspect.a034611

Davis, W., Endo, M., & Locke, J. C. W. (2022). Spatially specific mechanisms and functions of the plant circadian clock. *Plant Physiology*, *190*(2), 938–951. https://doi.org/10.1093/plphys/kiac236

Dixon, L. E., Knox, K., Kozma-Bognar, L., Southern, M. M., Pokhilko, A., & Millar, A. J. (2011). Temporal repression of core circadian genes is mediated through EARLY FLOWERING 3 in Arabidopsis. *Current Biology*, *21*(2), 120–125. https://doi.org/10.1016/j.cub.2010.12.013

Dodd, A. N., Salathia, N., Hall, A., Kévei, E., Tóth, Ŕ., Nagy, F., Hibberd, J. M., Millar, A. J., & Webb, A. A. R. (2005). Plant circadian clocks increase photosynthesis, growth, survival, and competitive advantage. *Science*, *309*(5734), 630–633. https://doi.org/10.1126/science.1115581

Dowson-Day, M. J., & Millar, A. J. (1999). Circadian dysfunction causes aberrant hypocotyl elongation patterns in Arabidopsis. *Plant*, *17*(1), 63–71. https://doi.org/10.1046/j.1365-313X.1999.00353.x

Farinas, B., & Mas, P. (2011). Functional implication of the MYB transcription factor RVE8/LCL5 in the circadian control of histone acetylation. *The Plant Journal*, *66*(2), 318–329. https://doi.org/10.1111/j.1365-313X.2011.04484.x

Fauser, F., Schiml, S., & Puchta, H. (2014). Both CRISPR/Cas-based nucleases and nickases can be used efficiently for genome engineering in *Arabidopsis thaliana*. *The Plant Journal*, *79*(2), 348–359. https://doi.org/10.1111/tpj.12554

Fornara, F., Panigrahi, K. C. S., Gissot, L., Sauerbrunn, N., Rühl, M., Jarillo, J. A., & Coupland, G. (2009). Arabidopsis DOF transcription factors act redundantly to reduce CONSTANS expression and are essential for a photoperiodic flowering response. *Developmental Cell*, *17*(1), 75–86. https://doi.org/10.1016/j.devcel.2009.06.015

Franklin, K. A., Lee, S. H., Patel, D., Kumar, S. V., Spartz, A. K., Gu, C., Ye, S., Yu, P., Breen, G., Cohen, J. D., Wigge, P. A., & Gray, W. M. (2011). PHYTOCHROME-INTERACTING FACTOR 4 (PIF4) regulates auxin biosynthesis at high temperature. *Proceedings of the National Academy of Sciences of the United States of America*, *108*(50), 20231–20235. https://doi.org/10.1073/pnas.1110682108

Gao, Y., & Zhao, Y. (2013). Epigenetic suppression of T-DNA insertion mutants in Arabidopsis. *Molecular Plant*, *6*(2), 539–545. https://doi.org/10.1093/mp/sss093

Gendron, J. M., Pruneda-Paz, J. L., Doherty, C. J., Gross, A. M., Kang, S. E., & Kay, S. A. (2012). Arabidopsis circadian clock protein, TOC1, is a DNA-binding transcription factor. *Proceedings of the National Academy of Sciences of the United States of America*, *109*(8), 3167–3172. https://doi.org/10.1073/pnas.1200355109

Graves, S., Piepho, H. P., & Sundar Dorai-Raj, L. S. (2019). *multcompView: Visualizations of paired comparisons*. https://CRAN.R-project.org/package=multcompView

Gray, J. A., Shalit-Kaneh, A., Chu, D. N., Hsu, P. Y., & Harmer, S. L. (2017). The REVEILLE clock genes inhibit growth of juvenile and adult plants by control of cell size. *Plant Physiology*, *173*(4), 2308–2322. https://doi.org/10.1104/pp.17.00109

Green, R. M., & Tobin, E. M. (1999). Loss of the circadian clock-associated protein 1 in Arabidopsis results in altered clock-regulated gene expression. *Proceedings of the National Academy of Sciences of the United States of America*, *96*(7), 4176–4179. https://doi.org/10.1073/pnas.96.7.4176

Haeussler, M., Schönig, K., Eckert, H., Eschstruth, A., Mianné, J., Renaud, J. B., Schneider-Maunoury, S., Shkumatava, A., Teboul, L., Kent, J., Joly, J. S., & Concordet, J. P. (2016). Evaluation of off-target and on-target scoring algorithms and integration into the guide RNA selection tool CRISPOR. *Genome Biology*, *17*(1), 148. https://doi.org/10.1186/s13059-016-1012-2

Hall, A., Bastow, R. M., Davis, S. J., Hanano, S., McWatters, H. G., Hibberd, V., Doyle, M. R., Sung, S., Halliday, K. J., Amasino, R. M., & Millar, A. J. (2003). The TIME FOR COFFEE gene maintains the amplitude and timing of Arabidopsis circadian clocks. *The Plant Cell*, *15*(11), 2719–2729. https://doi.org/10.1105/tpc.013730

Harmer, S. L., & Kay, S. A. (2005). Positive and negative factors confer phase-specific circadian regulation of transcription in Arabidopsis. *The Plant Cell*, *17*(7), 1926–1940. https://doi.org/10.1105/tpc.105.033035

Hartley, J. L., Temple, G. F., & Brasch, M. A. (2000). DNA cloning using in vitro site-specific recombination. *Genome Research*, *10*(11), 1788–1795. https://doi.org/10.1101/gr.143000

Hazen, S. P., Schultz, T. F., Pruneda-Paz, J. L., Borevitz, J. O., Ecker, J. R., & Kay, S. A. (2005). LUX ARRHYTHMO encodes a Myb domain protein essential for circadian rhythms. *Proceedings of the National Academy*

of Sciences of the United States of America, *102*(29), 10387–10392. https://doi.org/10.1073/pnas.0503029102

Helfer, A., Nusinow, D. A., Chow, B. Y., Gehrke, A. R., Bulyk, M. L., & Kay, S. A. (2011). LUX ARRHYTHMO encodes a nighttime repressor of circadian gene expression in the Arabidopsis core clock. *Current Biology*, *21*(2), 126–133. https://doi.org/10.1016/j.cub.2010.12.021

Hester, J., & Bryan, J. (2022). *glue: Interpreted string literals*. https://CRAN.R-project.org/package=glue

Hornitschek, P., Kohnen, M. V., Lorrain, S., Rougemont, J., Ljung, K., López-Vidriero, I., Franco-Zorrilla, J. M., Solano, R., Trevisan, M., Pradervand, S., Xenarios, I., & Fankhauser, C. (2012). Phytochrome interacting factors 4 and 5 control seedling growth in changing light conditions by directly controlling auxin signaling. *The Plant Journal*, *71*(5), 699–711. https://doi.org/10.1111/j.1365-313X.2012.05033.x

Hothorn, T., Bretz, F., & Westfall, P. (2008). Simultaneous inference in general parametric models. *Biometrical Journal*, *50*(3), 346–363. https://doi.org/10.1002/bimj.200810425

Hsu, P. Y., Devisetty, U. K., & Harmer, S. L. (2013). Accurate timekeeping is controlled by a cycling activator in Arabidopsis. *eLife*, *2*, e00473. https://doi.org/10.7554/eLife.00473

Hsu, P. Y., & Harmer, S. L. (2014). Wheels within wheels: The plant circadian system. *Trends in Plant Science*, *19*(4), 240–249. https://doi.org/10.1016/j.tplants.2013.11.007

Huang, W., Pérez-García, P., Pokhilko, A., Millar, A. J., Antoshechkin, I., Riechmann, J. L., & Mas, P. (2012). Mapping the core of the Arabidopsis circadian clock defines the network structure of the oscillator. *Science*, *336*(6077), 75–79. https://doi.org/10.1126/science.1219075

Kamioka, M., Takao, S., Suzuki, T., Taki, K., Higashiyama, T., Kinoshita, T., & Nakamichi, N. (2016). Direct repression of evening genes by CIRCADIAN CLOCK-ASSOCIATED1 in the Arabidopsis circadian clock. *The Plant Cell*, *28*(3), 696–711. https://doi.org/10.1105/tpc.15.00737

Kardailsky, I., Shukla, V. K., Ahn, J. H., Dagenais, N., Christensen, S. K., Nguyen, J. T., Chory, J., Harrison, M. J., & Weigel, D. (1999). Activation tagging of the floral inducer FT. *Science*, *286*(5446), 1962–1965. https://doi.org/10.1126/science.286.5446.1962

Kassambara, A. (2021). *rstatix: Pipe-friendly framework for basic statistical tests*. https://rpkgs.datanovia.com/rstatix/

Kobayashi, Y., Kaya, H., Goto, K., Iwabuchi, M., & Araki, T. (1999). A pair of related genes with antagonistic roles in mediating flowering signals. *Science*, *286*(5446), 1960–1962. https://doi.org/10.1126/science.286.5446.1960

Koini, M. A., Alvey, L., Allen, T., Tilley, C. A., Harberd, N. P., Whitelam, G. C., & Franklin, K. A. (2009). High temperature-mediated adaptations in plant architecture require the bHLH transcription factor PIF4. *Current Biology*, *19*(5), 408–413. https://doi.org/10.1016/j.cub.2009.01.046

Kunihiro, A., Yamashino, T., Nakamichi, N., Niwa, Y., Nakanishi, H., & Mizuno, T. (2011). PHYTOCHROME-INTERACTING FACTOR 4 and 5 (PIF4 and PIF5) activate the homeobox ATHB2 and auxin-inducible IAA29 genes in the coincidence mechanism underlying photoperiodic control of plant growth of *Arabidopsis thaliana*. *Plant & Cell Physiology*, *52*(8), 1315–1329. https://doi.org/10.1093/pcp/pcr076

Kuznetsova, A., Brockhoff, P. B., & Christensen, R. H. B. (2017). lmerTest package: Tests in linear mixed effects models. *Journal of Statistical Software*, *82*(13), 1–26. https://doi.org/10.18637/jss.v082.i13

Lenth, R. V. (2021). *emmeans: Estimated marginal means, aka least-squares means*. https://github.com/rvlenth/emmeans

Li, G., Siddiqui, H., Teng, Y., Lin, R., Wan, X. Y., Li, J., Lau, O. S., Ouyang, X., Dai, M., Wan, J., Devlin, P. F., Deng, X. W., & Wang, H. (2011). Coordinated transcriptional regulation underlying the circadian clock in Arabidopsis. *Nature Cell Biology*, *13*(5), 616–622. https://doi.org/10.1038/ncb2219

Locke, J. C. W., Southern, M. M., Kozma-Bognár, L., Hibberd, V., Brown, P. E., Turner, M. S., & Millar, A. J. (2005). Extension of a genetic network model by iterative experimentation and mathematical analysis. *Molecular Systems Biology*, *1*(1), 2005.0013. https://doi.org/10.1038/msb4100018

Lu, S. X., Knowles, S. M., Andronis, C., Ong, M. S., & Tobin, E. M. (2009). CIRCADIAN CLOCK ASSOCIATED1 and LATE ELONGATED HYPOCOTYL function synergistically in the circadian clock of Arabidopsis. *Plant Physiology*, *150*(2), 834–843. https://doi.org/10.1104/pp.108.133272

Maeda, A. E., & Nakamichi, N. (2022). Plant clock modifications for adapting flowering time to local environments. *Plant Physiology*, *190*(2), 952–967. https://doi.org/10.1093/plphys/kiac107

Maloof, J. N., Nozue, K., Mumbach, M. R., & Palmer, C. M. (2013). LeafJ: An ImageJ plugin for semi-automated leaf shape measurement. *Journal of Visualized Experiments*, *71*, e50028. https://doi.org/10.3791/50028

Marshall, C. M., Tartaglio, V., Duarte, M., & Harmon, F. G. (2016). The Arabidopsis sickle mutant exhibits altered circadian clock responses to cool temperatures and temperature-dependent alternative splicing. *The Plant Cell*, *28*(10), 2560–2575. https://doi.org/10.1105/tpc.16.00223

Martín, G., Rovira, A., Veciana, N., Soy, J., Toledo-Ortiz, G., Gommers, C. M. M., Boix, M., Henriques, R., Minguet, E. G., Alabadí, D., Halliday, K. J., Leivar, P., & Monte, E. (2018). Circadian waves of transcriptional repression shape PIF-regulated photoperiod-responsive growth in Arabidopsis. *Current Biology*, *28*(2), 311–318.e5. https://doi.org/10.1016/j.cub.2017.12.021

Martin-Tryon, E. L., Kreps, J. A., & Harmer, S. L. (2007). GIGANTEA acts in blue light signaling and has biochemically separable roles in circadian clock and flowering time regulation. *Plant Physiology*, *143*(1), 473–486. https://doi.org/10.1104/pp.106.088757

Más, P., Alabadí, D., Yanovsky, M. J., Oyama, T., & Kay, S. A. (2003). Dual role of TOC1 in the control of circadian and photomorphogenic responses in Arabidopsis. *The Plant Cell*, *15*(1), 223–236. https://doi.org/10.1105/tpc.006734

Michael, T. P., Salomé, P. A., Yu, H. J., Spencer, T. R., Sharp, E. L., McPeek, M. A., Alonso, J. M., Ecker, J. R., & McClung, C. R. (2003). Enhanced fitness conferred by naturally occurring variation in the circadian clock. *Science*, *302*(5647), 1049–1053. https://doi.org/10.1126/science.1082971

Mizoguchi, T., Wheatley, K., Hanzawa, Y., Wright, L., Mizoguchi, M., Song, H. R., Carré, I. A., & Coupland, G. (2002). LHY and CCA1 are partially redundant genes required to maintain circadian rhythms in Arabidopsis. *Developmental Cell*, *2*(5), 629–641. https://doi.org/10.1016/S1534-5807(02)00170-3

Monroe, J. G. (2017). *genemodel: Gene model plotting in R*. https://github.com/greymonroe/genemodel

Nagel, D. H., Doherty, C. J., Pruneda-Paz, J. L., Schmitz, R. J., Ecker, J. R., & Kay, S. A. (2015). Genome-wide identification of CCA1 targets uncovers an expanded clock network in Arabidopsis. *Proceedings of the National Academy of Sciences of the United States of America*, *112*(34), E4802–E4810. https://doi.org/10.1073/pnas.1513609112

Nakamichi, N., Kiba, T., Henriques, R., Mizuno, T., Chua, N. H., & Sakakibara, H. (2010). PSEUDO-RESPONSE REGULATORS 9, 7, and 5 are transcriptional repressors in the Arabidopsis circadian clock. *The Plant Cell*, *22*(3), 594–605. https://doi.org/10.1105/tpc.109.072892

Nakamichi, N., Kiba, T., Kamioka, M., Suzuki, T., Yamashino, T., Higashiyama, T., Sakakibara, H., & Mizuno, T. (2012). Transcriptional repressor PRR5 directly regulates clock-output pathways. *Proceedings of the National Academy of Sciences of the United States of*

America, *109*(42), 17123–17128. https://doi.org/10.1073/pnas.1205156109

Neuwirth, E. (2022). *RColorBrewer: ColorBrewer palettes*. https://CRAN.R-project.org/package=RColorBrewer

Niwa, Y., Ito, S., Nakamichi, N., Mizoguchi, T., Niinuma, K., Yamashino, T., & Mizuno, T. (2007). Genetic linkages of the circadian clock-associated genes, TOC1, CCA1 and LHY, in the photoperiodic control of flowering time in Arabidopsis thaliana. *Plant & Cell Physiology*, *48*(7), 925–937. https://doi.org/10.1093/pcp/pcm067

Nozue, K., Harmer, S. L., & Maloof, J. N. (2011). Genomic analysis of circadian clock-, light-, and growth-correlated genes reveals PHYTOCHROME-INTERACTING FACTOR5 as a modulator of auxin signaling in Arabidopsis. *Plant Physiology*, *156*(1), 357–372. https://doi.org/10.1104/pp.111.172684

Nusinow, D. A., Helfer, A., Hamilton, E. E., King, J. J., Imaizumi, T., Schultz, T. F., Farré, E. M., & Kay, S. A. (2011). The ELF4–ELF3–LUX complex links the circadian clock to diurnal control of hypocotyl growth. *Nature*, *475*(7356), 398–402. https://doi.org/10.1038/nature10182

Osabe, K., Harukawa, Y., Miura, S., & Saze, H. (2017). Epigenetic regulation of intronic transgenes in Arabidopsis. *Scientific Reports*, *7*(1), 45166. https://doi.org/10.1038/srep45166

Ouyang, Y., Andersson, C. R., Kondo, T., Golden, S. S., & Johnson, C. H. (1998). Resonating circadian clocks enhance fitness in cyanobacteria. *Proceedings of the National Academy of Sciences of the United States of America*, *95*(15), 8660–8664. https://doi.org/10.1073/pnas.95.15.8660

R Core Team. (2023). *R: A language and environment for statistical computing*. R Foundation for Statistical Computing, Vienna, Austria. https://www.R-project.org/

Rawat, R., Takahashi, N., Hsu, P. Y., Jones, M. A., Schwartz, J., Salemi, M. R., Phinney, B. S., & Harmer, S. L. (2011). REVEILLE8 and PSEUDO-REPONSE REGULATOR5 form a negative feedback loop within the Arabidopsis circadian clock. *PLoS Genetics*, *7*(3), e1001350. https://doi.org/10.1371/journal.pgen.1001350

Robinson, D., Hayes, A., & Couch, S. (2023). *broom: Convert statistical objects into tidy tibbles*. https://CRAN.R-project.org/package=broom

Rosbash, M. (2009). The implications of multiple circadian clock origins. *PLoS Biology*, *7*(3), e1000062. https://doi.org/10.1371/journal.pbio.1000062

Sandhu, K. S., Koirala, P. S., & Neff, M. M. (2013). The ben1-1 brassinosteroid-catabolism mutation is unstable due to epigenetic modifications of the intronic T-DNA insertion. *G3*, *3*(9), 1587–1595. https://doi.org/10.1534/g3.113.006353

Sarkar, D. (2008). *Lattice: Multivariate data visualization with R*. Springer. http://lmdvr.r-forge.r-project.org, https://doi.org/10.1007/978-0-387-75969-2

Schneider, C. A., Rasband, W. S., & Eliceiri, K. W. (2012). NIH image to ImageJ: 25 years of image analysis. *Nature Methods*, *9*(7), 671–675. https://doi.org/10.1038/nmeth.2089

Shalit-Kaneh, A., Kumimoto, R. W., Filkov, V., & Harmer, S. L. (2018). Multiple feedback loops of the Arabidopsis circadian clock provide rhythmic robustness across environmental conditions. *Proceedings of the National Academy of Sciences of the United States of America*, *115*(27), 7147–7152. https://doi.org/10.1073/pnas.1805524115

Song, Y. H., Shim, J. S., Kinmonth-Schultz, H. A., & Imaizumi, T. (2015). Photoperiodic flowering: Time measurement mechanisms in leaves. *Annual Review of Plant Biology*, *66*(1), 441–464. https://doi.org/10.1146/annurev-arplant-043014-115555

Soy, J., Leivar, P., González-Schain, N., Martín, G., Diaz, C., Sentandreu, M., al-Sady, B., Quail, P. H., & Monte, E. (2016). Molecular convergence of clock and photosensory pathways through PIF3–TOC1 interaction and co-occupancy of target promoters. *Proceedings of the National Academy of Sciences of the United States of America*, *113*(17), 4870–4875. https://doi.org/10.1073/pnas.1603745113

Spoelstra, K., Wikelski, M., Daan, S., Loudon, A. S. I., & Hau, M. (2016). Natural selection against a circadian clock gene mutation in mice. *Proceedings of the National Academy of Sciences of the United States of America*, *113*(3), 686–691. https://doi.org/10.1073/pnas.1516442113

Steindler, C., Matteucci, A., Sessa, G., Weimar, T., Ohgishi, M., Aoyama, T., Morelli, G., & Ruberti, I. (1999). Shade avoidance responses are mediated by the ATHB-2 HD-zip protein, a negative regulator of gene expression. *Development*, *126*(19), 4235–4245. https://doi.org/10.1242/dev.126.19.4235

Strayer, C., Oyama, T., Schultz, T. F., Raman, R., Somers, D. E., Más, P., Panda, S., Kreps, J. A., & Kay, S. A. (2000). Cloning of the Arabidopsis clock gene TOC1, an autoregulatory response regulator homolog. *Science*, *289*(5480), 768–771. https://doi.org/10.1126/science.289.5480.768

Sun, J., Qi, L., Li, Y., Chu, J., & Li, C. (2012). PIF4–mediated activation of YUCCA8 expression integrates temperature into the auxin pathway in regulating Arabidopsis hypocotyl growth. *PLoS Genetics*, *8*(3), e1002594. https://doi.org/10.1371/journal.pgen.1002594

Tao, Y., Ferrer, J. L., Ljung, K., Pojer, F., Hong, F., Long, J. A., Li, L., Moreno, J. E., Bowman, M. E., Ivans, L. J., Cheng, Y., Lim, J., Zhao, Y., Ballaré, C. L., Sandberg, G., Noel, J. P., & Chory, J. (2008). Rapid synthesis of auxin via a new tryptophan-dependent pathway is required for shade avoidance in plants. *Cell*, *133*(1), 164–176. https://doi.org/10.1016/j.cell.2008.01.049

Wang, Z. Y., & Tobin, E. M. (1998). Constitutive expression of the CIRCADIAN CLOCK ASSOCIATED 1 (CCA1) gene disrupts circadian rhythms and suppresses its own expression. *Cell*, *93*(7), 1207–1217. https://doi.org/10.1016/S0092-8674(00)81464-6

Wickham, H., Averick, M., Bryan, J., Chang, W., McGowan, L., François, R., Grolemund, G., Hayes, A., Henry, L., Hester, J., Kuhn, M., Pedersen, T., Miller, E., Bache, S., Müller, K., Ooms, J., Robinson, D., Seidel, D., Spinu, V., … Yutani, H. (2019). Welcome to the tidyverse. *Journal of Open Source Software*, *4*(43), 1686. https://doi.org/10.21105/joss.01686

Wilke, C. O. (2020). *cowplot: Streamlined plot theme and plot annotations for ggplot2*. https://CRAN.R-project.org/package=cowplot

Wilke, C. O. (2022). *ggtext: Improved text rendering support for ggplot2*. https://CRAN.R-project.org/package=ggtext

Xie, K., Minkenberg, B., & Yang, Y. (2015). Boosting CRISPR/Cas9 multiplex editing capability with the endogenous tRNA-processing system. *Proceedings of the National Academy of Sciences of the United States of America*, *112*(11), 3570–3575. https://doi.org/10.1073/pnas.1420294112

Xue, W., Ruprecht, C., Street, N., Hematy, K., Chang, C., Frommer, W. B., Persson, S., & Niittylä, T. (2012). Paramutation-like interaction of T-DNA loci in Arabidopsis. *PLoS ONE*, *7*(12), e51651. https://doi.org/10.1371/journal.pone.0051651

Yakir, E., Hilman, D., Kron, I., Hassidim, M., Melamed-Book, N., & Green, R. M. (2009). Posttranslational regulation of CIRCADIAN CLOCK ASSOCIATED1 in the circadian oscillator of Arabidopsis. *Plant Physiology*, *150*(2), 844–857. https://doi.org/10.1104/pp.109.137414

Yuan, L., Yu, Y., Liu, M., Song, Y., Li, H., Sun, J., Wang, Q., Xie, Q., Wang, L., & Xu, X. (2021). BBX19 fine-tunes the circadian rhythm by interacting with PSEUDO-RESPONSE REGULATOR proteins to facilitate their repressive effect on morning-phased clock genes. *The Plant Cell*, *33*(8), 2602–2617. https://doi.org/10.1093/plcell/koab133

Zhang, Y., Pfeiffer, A., Tepperman, J. M., Dalton-Roesler, J., Leivar, P., Gonzalez Grandio, E., & Quail, P. H. (2020). Central clock components modulate plant shade avoidance by directly repressing transcriptional activation activity of PIF proteins. *Proceedings of the National Academy of Sciences of the United States of America*, *117*(6), 3261–3269. https://doi.org/10.1073/pnas.1918317117

Zhang, C., Xie, Q., Anderson, R. G., Ng, G., Seitz, N. C., Peterson, T., McClung, C., McDowell, J., Kong, D., Kwak, J. M., & Lu, H. (2013). Crosstalk between the circadian clock and innate immunity in Arabidopsis. *PLoS Pathogens*, *9*(6), e1003370. https://doi.org/10.1371/journal.ppat.1003370

SUPPORTING INFORMATION

Additional supporting information can be found online in the Supporting Information section at the end of this article.

How to cite this article: Hughes, C. L., & Harmer, S. L. (2023). Myb-like transcription factors have epistatic effects on circadian clock function but additive effects on plant growth. *Plant Direct*, *7*(10), e533. https://doi.org/10.1002/pld3.533